

# Ecosystem size and complexity dictate riverine biodiversity

## Supplementary Information for:

Akira Terui\*      Seoghyun Kim\*      Christine L. Dolph<sup>†</sup>      Taku Kadoya<sup>‡</sup>  
Yusuke Miyazaki<sup>§</sup>

## Contents

<b>Fish community data</b>	<b>1</b>
Hokkaido, Japan . . . . .	1
Midwest, US . . . . .	2
<b>Tables</b>	<b>3</b>
Table S1 Species list in Hokkaido, Japan . . . . .	3
<b>Figures</b>	<b>5</b>
Figure S1 Influence of ecosystem size ( $p_d = 0.1, \sigma_h = 1, \sigma_l = 0.01$ ) . . . . .	5
Figure S2 Influence of ecosystem size ( $p_d = 0.1, \sigma_h = 1, \sigma_l = 1$ ) . . . . .	6
Figure S3 Influence of ecosystem size ( $p_d = 0.1, \sigma_h = 0.01, \sigma_l = 0.01$ ) . . . . .	7
Figure S4 Influence of ecosystem size ( $p_d = 0.1, \sigma_h = 0.01, \sigma_l = 1$ ) . . . . .	8
Figure S5 Influence of ecosystem size ( $p_d = 0.01, \sigma_h = 1, \sigma_l = 1$ ) . . . . .	9
Figure S6 Influence of ecosystem size ( $p_d = 0.01, \sigma_h = 0.01, \sigma_l = 0.01$ ) . . . . .	10
Figure S7 Influence of ecosystem size ( $p_d = 0.01, \sigma_h = 0.01, \sigma_l = 1$ ) . . . . .	11
Figure S8 Influence of ecosystem complexity ( $p_d = 0.1, \sigma_h = 1, \sigma_l = 0.01$ ) . . . . .	12
Figure S9 Influence of ecosystem complexity ( $p_d = 0.1, \sigma_h = 1, \sigma_l = 1$ ) . . . . .	13
Figure S10 Influence of ecosystem complexity ( $p_d = 0.1, \sigma_h = 0.01, \sigma_l = 0.01$ ) . . . . .	14
Figure S11 Influence of ecosystem complexity ( $p_d = 0.1, \sigma_h = 0.01, \sigma_l = 1$ ) . . . . .	15
Figure S12 Influence of ecosystem complexity ( $p_d = 0.01, \sigma_h = 1, \sigma_l = 1$ ) . . . . .	16
Figure S13 Influence of ecosystem complexity ( $p_d = 0.01, \sigma_h = 0.01, \sigma_l = 0.01$ ) . . . . .	17
Figure S14 Influence of ecosystem complexity ( $p_d = 0.01, \sigma_h = 0.01, \sigma_l = 1$ ) . . . . .	18
<b>References</b>	<b>19</b>

## Fish community data

### Hokkaido, Japan

We used data from the Hokkaido Freshwater Fish Database HFish<sup>1</sup>, monitoring data at protected watersheds<sup>2,3</sup>, and primary data collected from literature<sup>4</sup>, which collectively cover the entire Hokkaido island. Data were collected from summer to fall. We screened data through the following procedure:

1. We listed recorded fish species and re-organized species names to be consistent across the data sets.

---

\*Department of Biology, University of North Carolina at Greensboro

<sup>†</sup>Department of Ecology, Evolution and Behavior, University of Minnesota

<sup>‡</sup>National Institute for Environmental Studies

<sup>§</sup>Shiraume Gakuen University

2. We selected sampling sites based on the following criteria: (1) surveys were conducted with netting and/or electrofishing, (2) surveys were designed to collect a whole fish community, (3) sites contained reliable coordinates (sites with coordinates identical at 3 decimal degrees were treated as the same site), and (4) sites did not involve unidentified species that are rarely observed in the data set ( $< 100$  sites occurrence).
3. For sites with multiple visits (i.e., temporal replicates), we used the latest-year observation at each sampling site to minimize variation in sampling efforts among sites. Surveys that occurred in the same year were aggregated into a single observation.
4. We confined sites to those with the latest observation year of  $\geq 1990$ . Although the data set contained observations from 1953, we added this restriction to align the observation period with the data set in the Midwest, US.
5. Four genera (Lethenteron, Pungitius, Rhinogobius, and Tribolodon) were treated as species groups (i.e., spp.) as taxonomic resolutions varied greatly among data sources.

## Midwest, US

We assembled fish community data collected by the Iowa Department of Natural Resources, Illinois Environmental Protection Agency and Illinois Department of Natural Resources, Minnesota Pollution Control Agency, and Wisconsin Department of Natural Resources. These data sets cover most of Upper Mississippi (HUC 2, region 07) and the part of Great Lakes (HUC 2, region 04), Missouri (HUC 2, region 10), and Ohio (HUC 2, region 05). Data were collected from summer to fall with electrofishing (backpack, barge-type, or boat-mounted) and supplemental netting at some locations. We screened data through the following procedure:

1. We used data of the Upper Mississippi (HUC 2, region 07) and Great Lakes basins (HUC 2, region 04) as most sites are included in these regions.
2. We removed records of unidentified species, hybrid species, and commercial species that are apparently absent in the wild (e.g., goldfish).
3. We used the latest observation at each sampling site to minimize variation in sampling efforts among sites.

# Tables

**Table S1 Species list in Hokkaido, Japan**

Species list in Hokkaido, Japan. Species are ordered alphabetically.

Species	Number of sites present
<i>Acanthogobius lactipes</i>	87
<i>Anguilla japonica</i>	1
<i>Carassius buergeri</i> subsp. 2	5
<i>Carassius cuvieri</i>	32
<i>Carassius</i> sp.	240
<i>Channa argus</i>	3
<i>Cottus amblystomopsis</i>	65
<i>Cottus hangiongensis</i>	161
<i>Cottus nozawae</i>	918
<i>Cottus</i> sp. ME	25
<i>Cyprinus carpio</i>	56
<i>Gasterosteus aculeatus</i>	228
<i>Gnathopogon caerulescens</i>	1
<i>Gnathopogon elongatus elongatus</i>	7
<i>Gymnogobius breunigii</i>	56
<i>Gymnogobius castaneus</i> complex	178
<i>Gymnogobius opperiens</i>	122
<i>Gymnogobius petschiliensis</i>	2
<i>Gymnogobius urotaenia</i>	433
<i>Hucho perryi</i>	63
<i>Hypomesus nipponensis</i>	228
<i>Hypomesus olidus</i>	12
<i>Lefua nikkonis</i>	24
<i>Lethenteron</i> spp.	863
<i>Leucopsarion petersii</i>	4
<i>Luciogobius guttatus</i>	17
<i>Misgurnus anguillicaudatus</i>	245
<i>Noemacheilus barbatulus</i>	1750
<i>Oncorhynchus gorboscha</i>	43
<i>Oncorhynchus keta</i>	211
<i>Oncorhynchus masou masou</i>	1667
<i>Oncorhynchus mykiss</i>	489
<i>Oncorhynchus nerka</i>	6
<i>Opsariichthys platypus</i>	1
<i>Osmerus dentex</i>	13
<i>Phoxinus phoxinus sachalinensis</i>	80
<i>Plecoglossus altivelis altivelis</i>	157
<i>Pseudorasbora parva</i>	104
<i>Pungitius</i> spp.	347
<i>Rhinogobius</i> spp.	244
<i>Rhodeus ocellatus ocellatus</i>	32
<i>Salangichthys microdon</i>	20
<i>Salmo trutta</i>	15
<i>Salvelinus fontinalis</i>	2
<i>Salvelinus leucomaenis leucomaenis</i>	790
<i>Salvelinus malma</i>	282
<i>Salvelinus malma miyabei</i>	2

Species	Number of sites present
<i>Silurus asotus</i>	7
<i>Spirinchus lanceolatus</i>	10
<i>Tribolodon</i> spp.	1410
<i>Tridentiger brevispinis</i>	155
<i>Tridentiger obscurus</i>	8

## Figures

**Figure S1 Influence of ecosystem size ( $p_d = 0.1$ ,  $\sigma_h = 1$ ,  $\sigma_l = 0.01$ )**

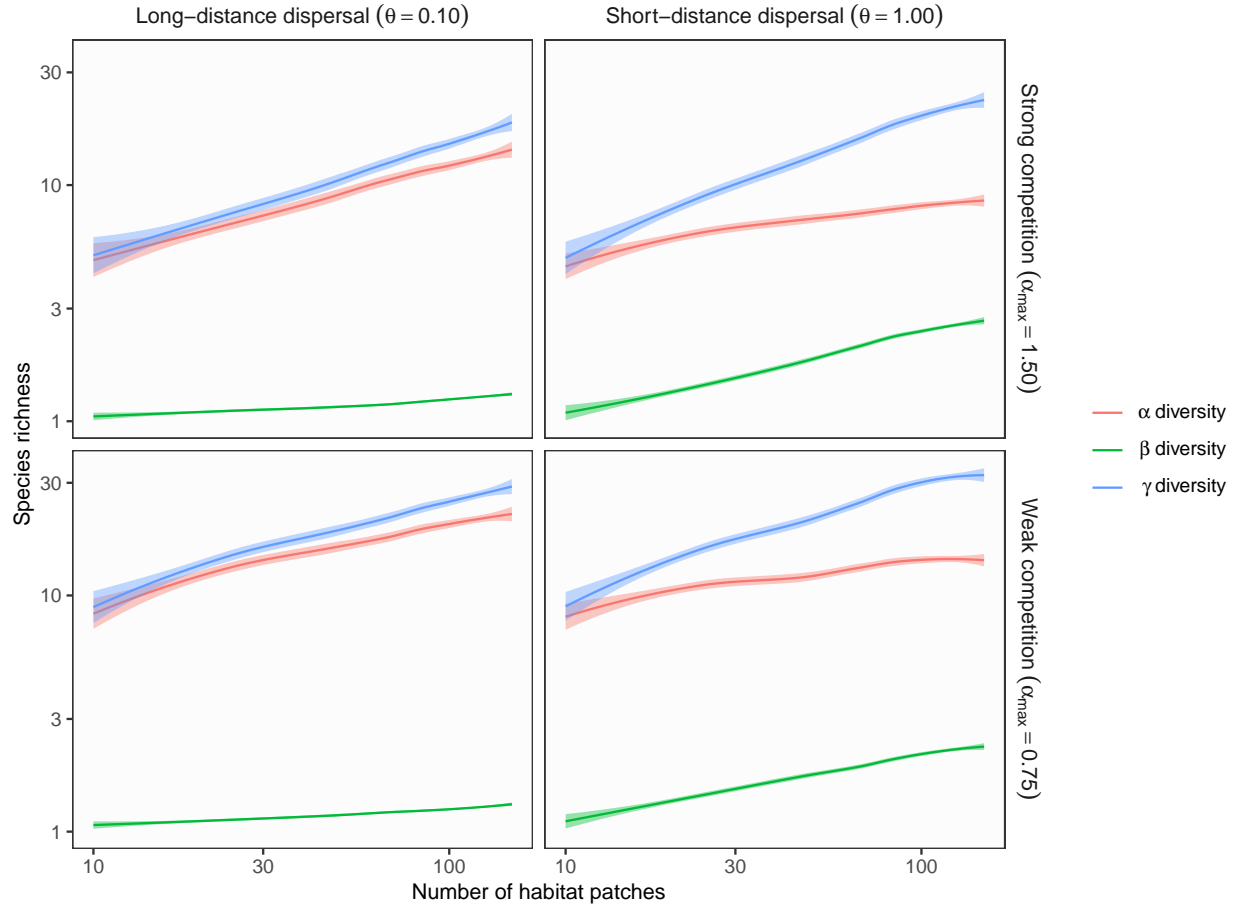


**Figure S1** Theoretical predictions for ecosystem size influences (the number of habitat patches) on  $\alpha$ ,  $\beta$ , and  $\gamma$  diversity in branching networks. In this simulation, environmental variation at headwaters ( $\sigma_h$ ) exceeds local environmental noise ( $\sigma_l$ ). Lines and shades are loess curves fitted to simulated data and its 95% confidence intervals. Each panel represents different ecological scenarios under which metacommunity dynamics were simulated. Rows represent different competition strength. Competitive coefficients ( $\alpha_{ij}$ ) were varied randomly from 0 to 1.5 (top, strong competition) or 0.75 (bottom, weak competition). Columns represent different dispersal scenarios. Two dispersal parameters were chosen to simulate scenarios with long-distance (the rate parameter of an exponential dispersal kernel  $\theta = 0.10$ ) and short-distance dispersal ( $\theta = 1.0$ ). Other parameters are as follows: dispersal probability  $p_d = 0.1$ ; environmental variation at headwaters  $\sigma_h = 1$ ; local environmental noise  $\sigma_l = 0.01$ .

**Figure S2 Influence of ecosystem size ( $p_d = 0.1$ ,  $\sigma_h = 1$ ,  $\sigma_l = 1$ )**

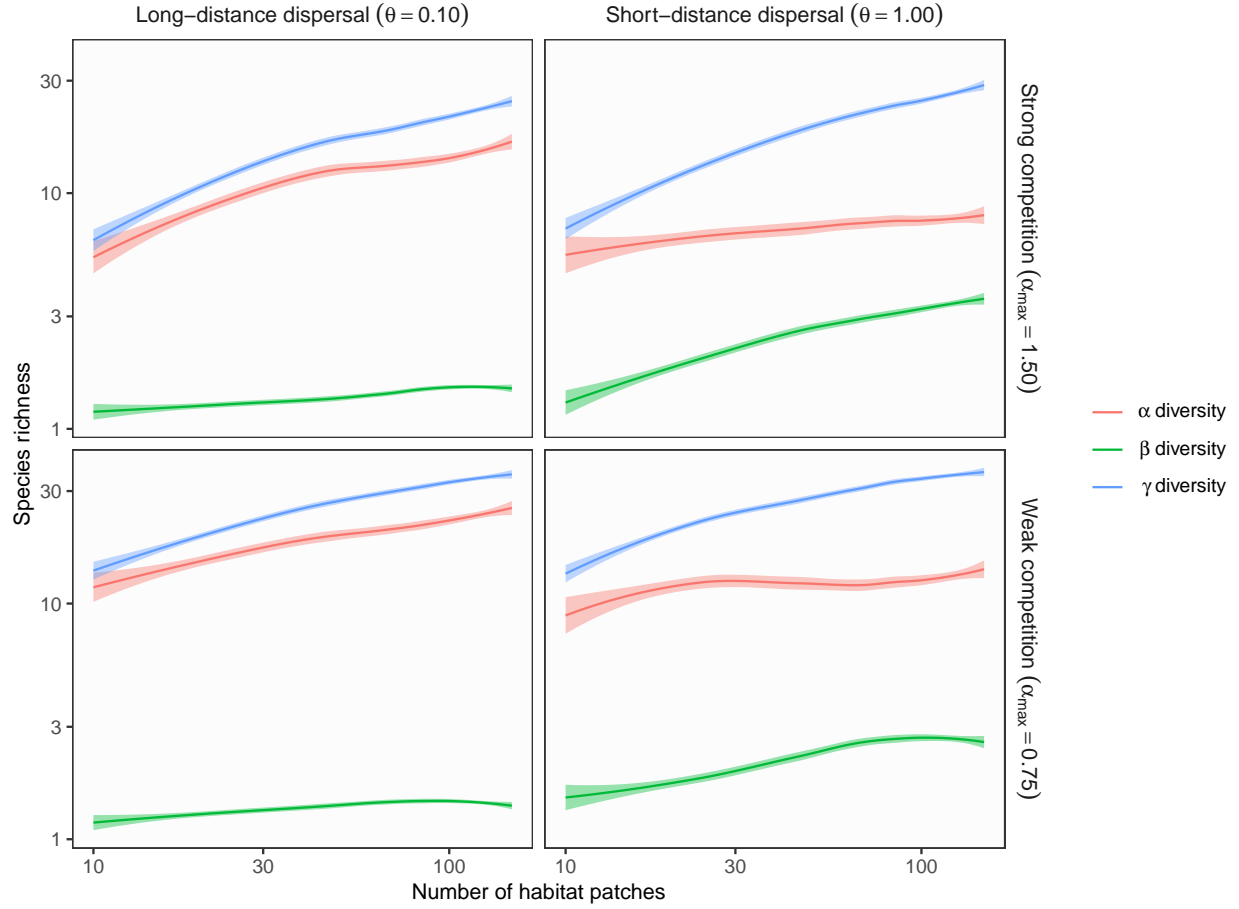


**Figure S2** Theoretical predictions for ecosystem size influences (the number of habitat patches) on  $\alpha$ ,  $\beta$ , and  $\gamma$  diversity in branching networks. In this simulation, environmental variation at headwaters ( $\sigma_h$ ) is equal to local environmental noise ( $\sigma_l$ ). Lines and shades are loess curves fitted to simulated data and its 95% confidence intervals. Each panel represents different ecological scenarios under which metacommunity dynamics were simulated. Rows represent different competition strength. Competitive coefficients ( $\alpha_{ij}$ ) were varied randomly from 0 to 1.5 (top, strong competition) or 0.75 (bottom, weak competition). Columns represent different dispersal scenarios. Two dispersal parameters were chosen to simulate scenarios with long-distance (the rate parameter of an exponential dispersal kernel  $\theta = 0.10$ ) and short-distance dispersal ( $\theta = 1.0$ ). Other parameters are as follows: dispersal probability  $p_d = 0.1$ ; environmental variation at headwaters  $\sigma_h = 1$ ; local environmental noise  $\sigma_l = 1$ .

**Figure S3 Influence of ecosystem size ( $p_d = 0.1$ ,  $\sigma_h = 0.01$ ,  $\sigma_l = 0.01$ )**

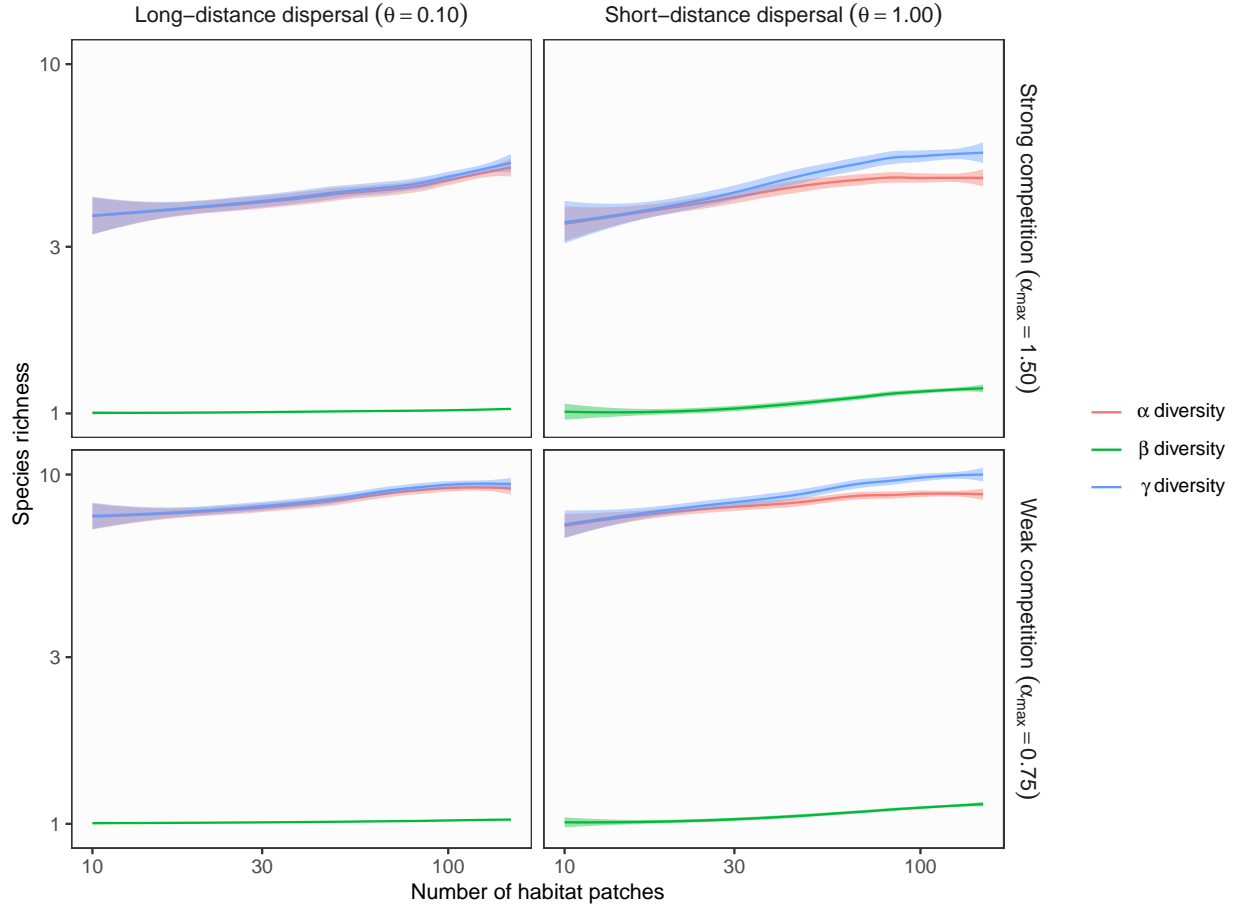


**Figure S3** Theoretical predictions for ecosystem size influences (the number of habitat patches) on  $\alpha$ ,  $\beta$ , and  $\gamma$  diversity in branching networks. In this simulation, environmental variation at headwaters ( $\sigma_h$ ) is equal to local environmental noise ( $\sigma_l$ ). Lines and shades are loess curves fitted to simulated data and its 95% confidence intervals. Each panel represents different ecological scenarios under which metacommunity dynamics were simulated. Rows represent different competition strength. Competitive coefficients ( $\alpha_{ij}$ ) were varied randomly from 0 to 1.5 (top, strong competition) or 0.75 (bottom, weak competition). Columns represent different dispersal scenarios. Two dispersal parameters were chosen to simulate scenarios with long-distance (the rate parameter of an exponential dispersal kernel  $\theta = 0.10$ ) and short-distance dispersal ( $\theta = 1.0$ ). Other parameters are as follows: dispersal probability  $p_d = 0.1$ ; environmental variation at headwaters  $\sigma_h = 0.01$ ; local environmental noise  $\sigma_l = 0.01$ .

**Figure S4 Influence of ecosystem size ( $p_d = 0.1$ ,  $\sigma_h = 0.01$ ,  $\sigma_l = 1$ )**

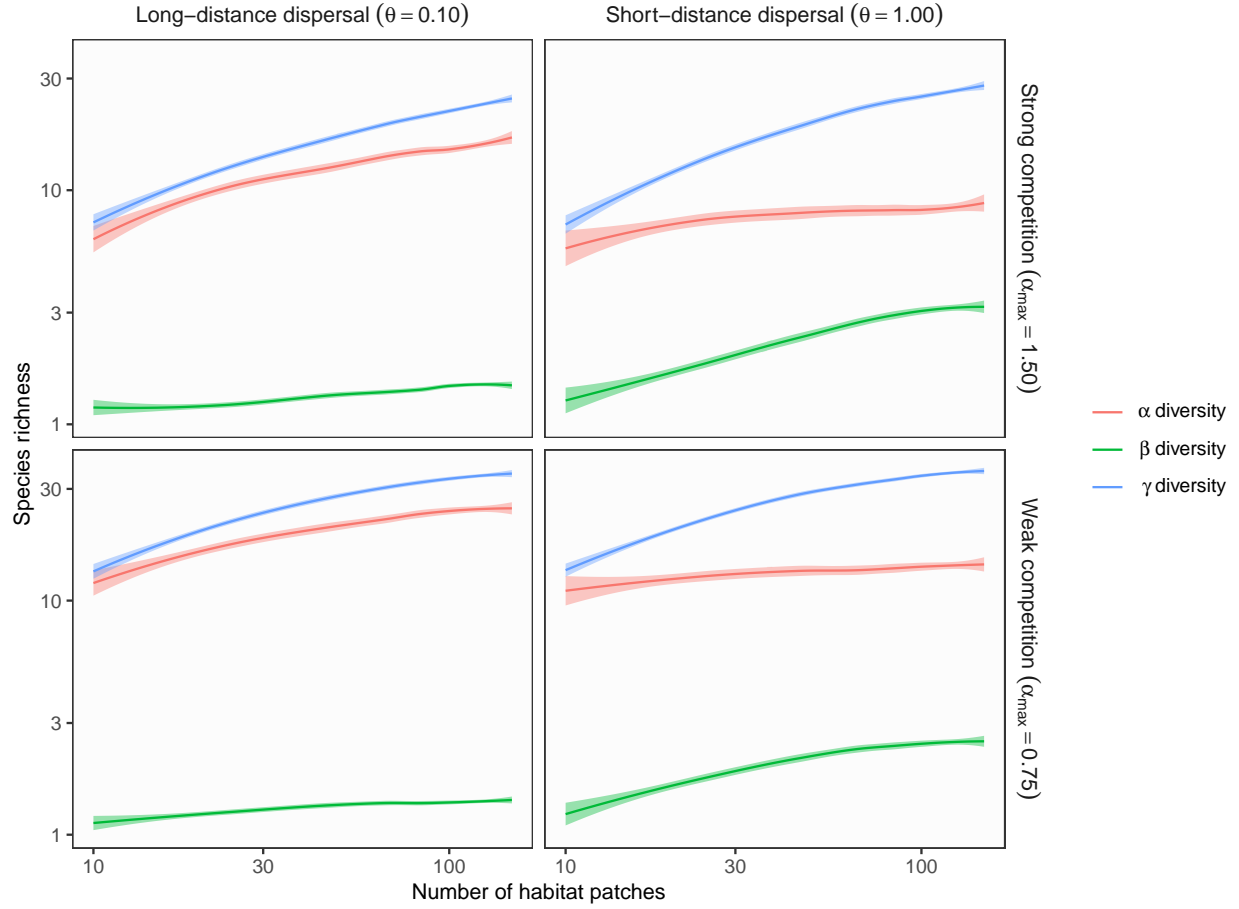


**Figure S4** Theoretical predictions for ecosystem size influences (the number of habitat patches) on  $\alpha$ ,  $\beta$ , and  $\gamma$  diversity in branching networks. In this simulation, environmental variation at headwaters ( $\sigma_h$ ) is less than local environmental noise ( $\sigma_l$ ). Lines and shades are loess curves fitted to simulated data and its 95% confidence intervals. Each panel represents different ecological scenarios under which metacommunity dynamics were simulated. Rows represent different competition strength. Competitive coefficients ( $\alpha_{ij}$ ) were varied randomly from 0 to 1.5 (top, strong competition) or 0.75 (bottom, weak competition). Columns represent different dispersal scenarios. Two dispersal parameters were chosen to simulate scenarios with long-distance (the rate parameter of an exponential dispersal kernel  $\theta = 0.10$ ) and short-distance dispersal ( $\theta = 1.0$ ). Other parameters are as follows: dispersal probability  $p_d = 0.1$ ; environmental variation at headwaters  $\sigma_h = 0.01$ ; local environmental noise  $\sigma_l = 1$ .



**Figure S5 Influence of ecosystem size ( $p_d = 0.01$ ,  $\sigma_h = 1$ ,  $\sigma_l = 1$ )**

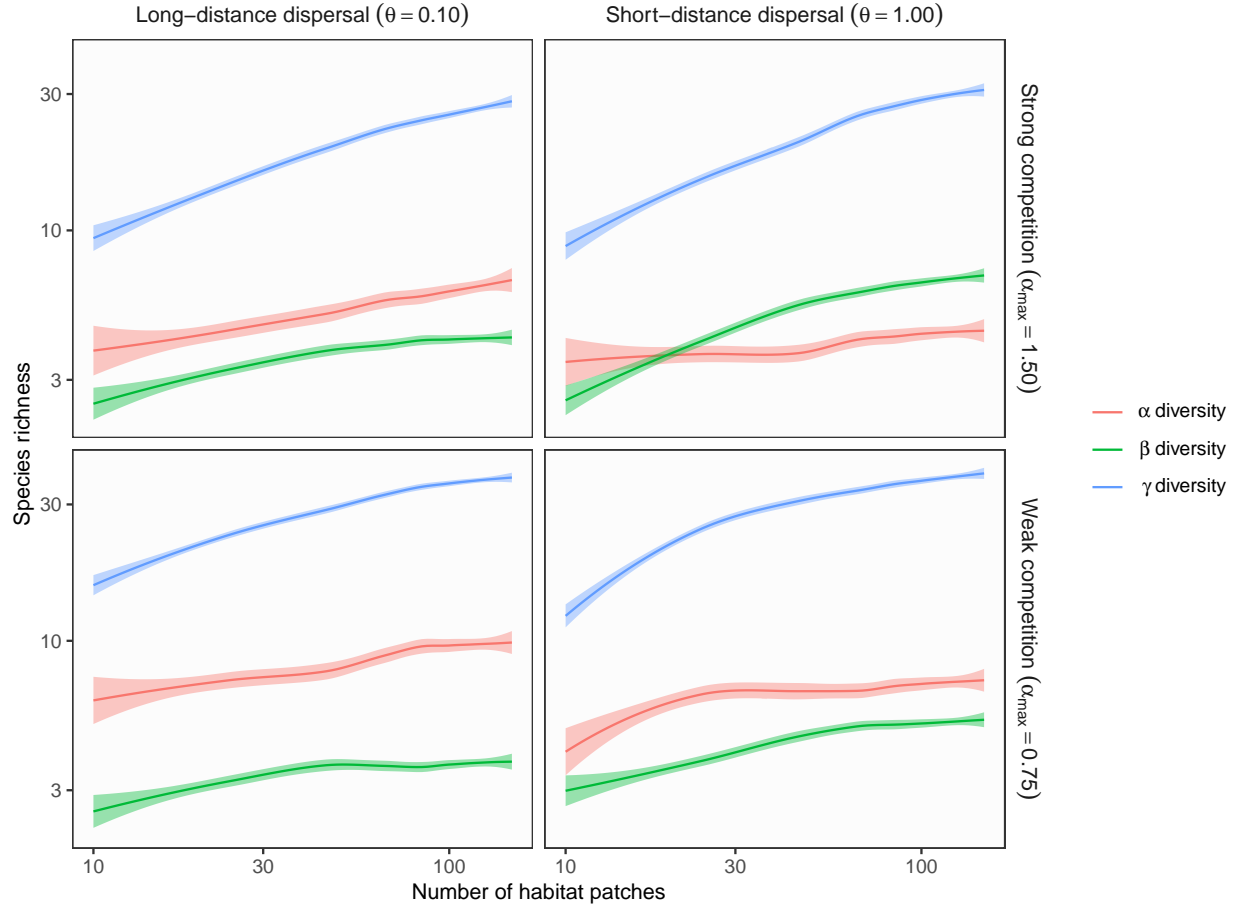


**Figure S5** Theoretical predictions for ecosystem size influences (the number of habitat patches) on  $\alpha$ ,  $\beta$ , and  $\gamma$  diversity in branching networks. In this simulation, environmental variation at headwaters ( $\sigma_h$ ) is equal to local environmental noise ( $\sigma_l$ ). Lines and shades are loess curves fitted to simulated data and its 95% confidence intervals. Each panel represents different ecological scenarios under which metacommunity dynamics were simulated. Rows represent different competition strength. Competitive coefficients ( $\alpha_{ij}$ ) were varied randomly from 0 to 1.5 (top, strong competition) or 0.75 (bottom, weak competition). Columns represent different dispersal scenarios. Two dispersal parameters were chosen to simulate scenarios with long-distance (the rate parameter of an exponential dispersal kernel  $\theta = 0.10$ ) and short-distance dispersal ( $\theta = 1.0$ ). Other parameters are as follows: dispersal probability  $p_d = 0.01$ ; environmental variation at headwaters  $\sigma_h = 1$ ; local environmental noise  $\sigma_l = 1$ .

**Figure S6 Influence of ecosystem size ( $p_d = 0.01$ ,  $\sigma_h = 0.01$ ,  $\sigma_l = 0.01$ )**

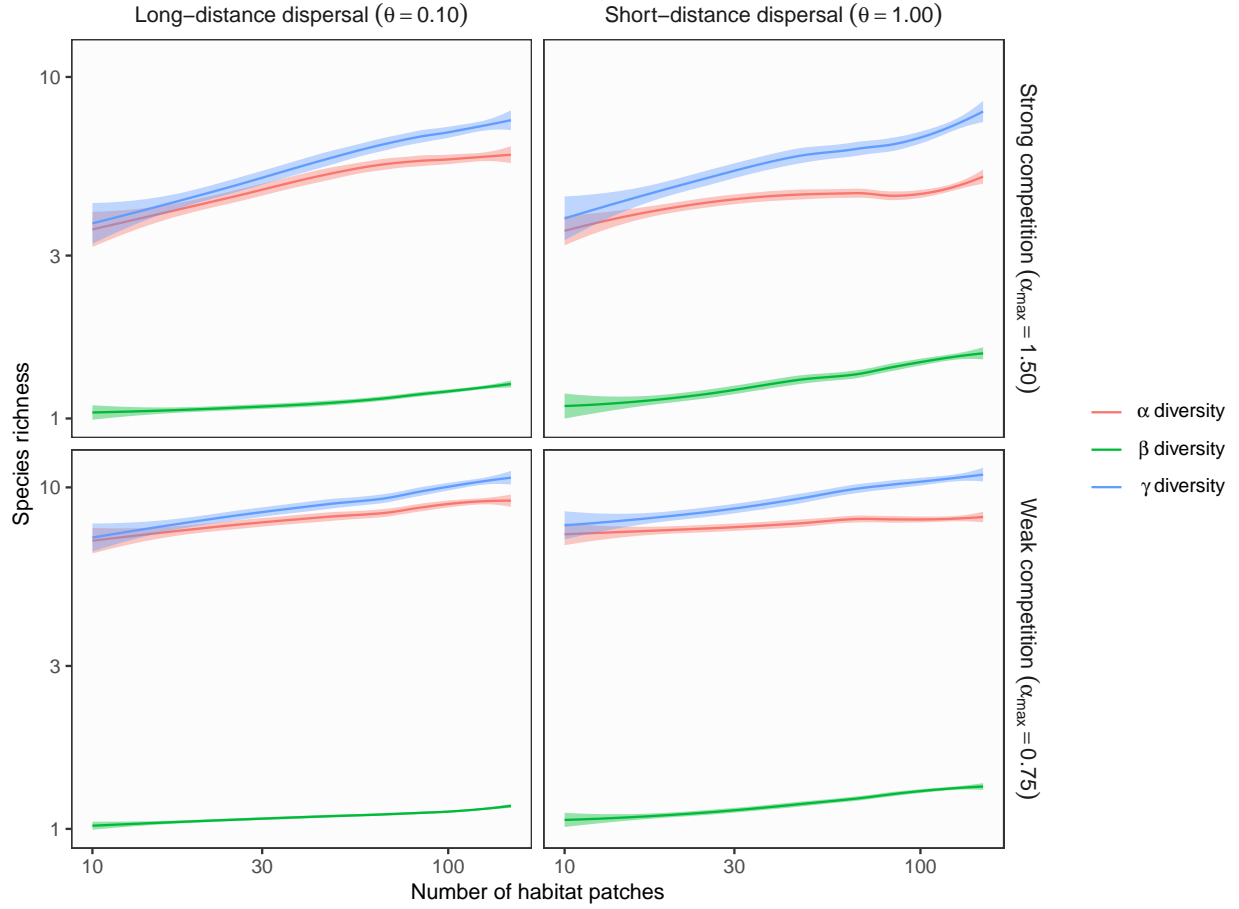


**Figure S6** Theoretical predictions for ecosystem size influences (the number of habitat patches) on  $\alpha$ ,  $\beta$ , and  $\gamma$  diversity in branching networks. In this simulation, environmental variation at headwaters ( $\sigma_h$ ) is equal to local environmental noise ( $\sigma_l$ ). Lines and shades are loess curves fitted to simulated data and its 95% confidence intervals. Each panel represents different ecological scenarios under which metacommunity dynamics were simulated. Rows represent different competition strength. Competitive coefficients ( $\alpha_{ij}$ ) were varied randomly from 0 to 1.5 (top, strong competition) or 0.75 (bottom, weak competition). Columns represent different dispersal scenarios. Two dispersal parameters were chosen to simulate scenarios with long-distance (the rate parameter of an exponential dispersal kernel  $\theta = 0.10$ ) and short-distance dispersal ( $\theta = 1.0$ ). Other parameters are as follows: dispersal probability  $p_d = 0.01$ ; environmental variation at headwaters  $\sigma_h = 0.01$ ; local environmental noise  $\sigma_l = 0.01$ .

**Figure S7 Influence of ecosystem size ( $p_d = 0.01$ ,  $\sigma_h = 0.01$ ,  $\sigma_l = 1$ )**

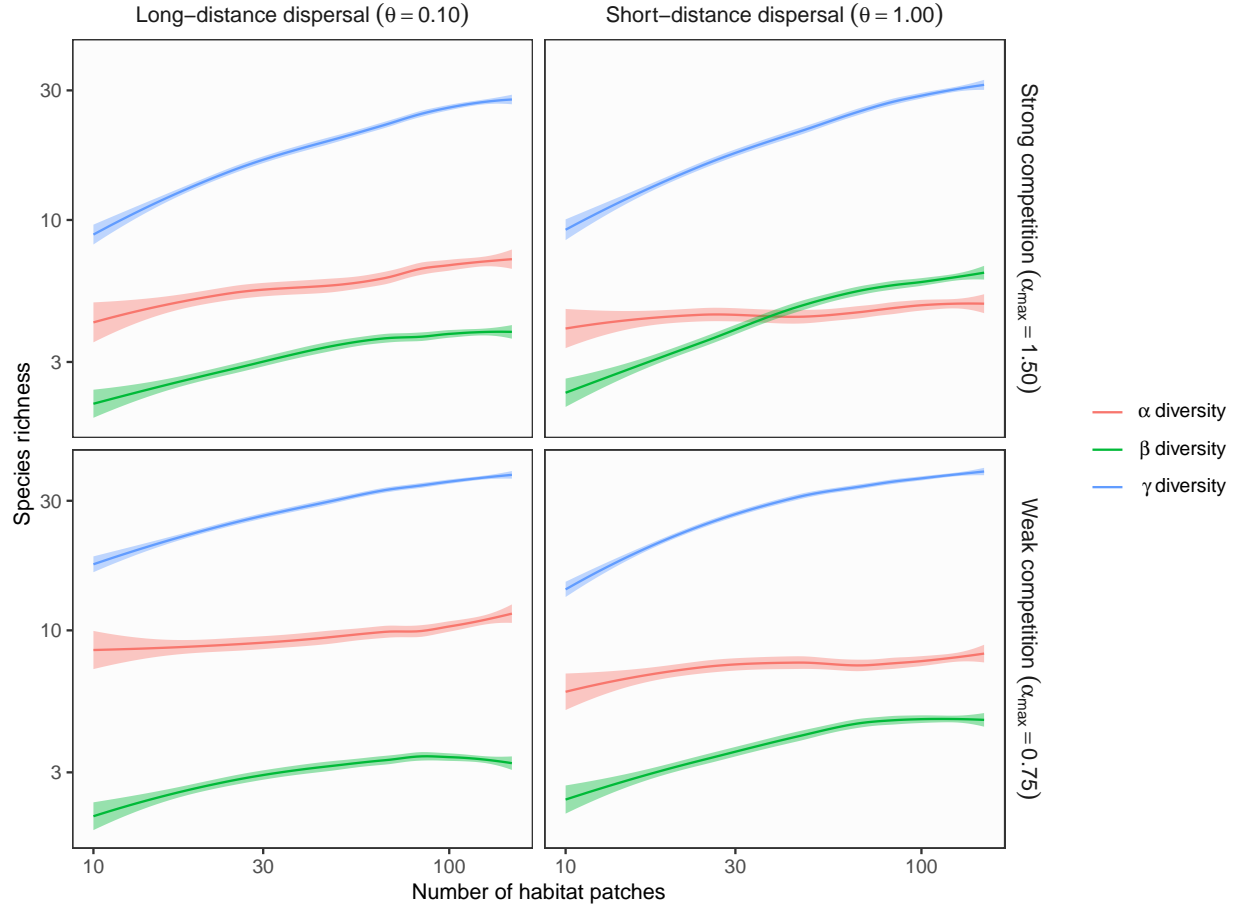


**Figure S7** Theoretical predictions for ecosystem size influences (the number of habitat patches) on  $\alpha$ ,  $\beta$ , and  $\gamma$  diversity in branching networks. In this simulation, environmental variation at headwaters ( $\sigma_h$ ) is less than local environmental noise ( $\sigma_l$ ). Lines and shades are loess curves fitted to simulated data and its 95% confidence intervals. Each panel represents different ecological scenarios under which metacommunity dynamics were simulated. Rows represent different competition strength. Competitive coefficients ( $\alpha_{ij}$ ) were varied randomly from 0 to 1.5 (top, strong competition) or 0.75 (bottom, weak competition). Columns represent different dispersal scenarios. Two dispersal parameters were chosen to simulate scenarios with long-distance (the rate parameter of an exponential dispersal kernel  $\theta = 0.10$ ) and short-distance dispersal ( $\theta = 1.0$ ). Other parameters are as follows: dispersal probability  $p_d = 0.01$ ; environmental variation at headwaters  $\sigma_h = 0.01$ ; local environmental noise  $\sigma_l = 1$ .

**Figure S8 Influence of ecosystem complexity ( $p_d = 0.1$ ,  $\sigma_h = 1$ ,  $\sigma_l = 0.01$ )**

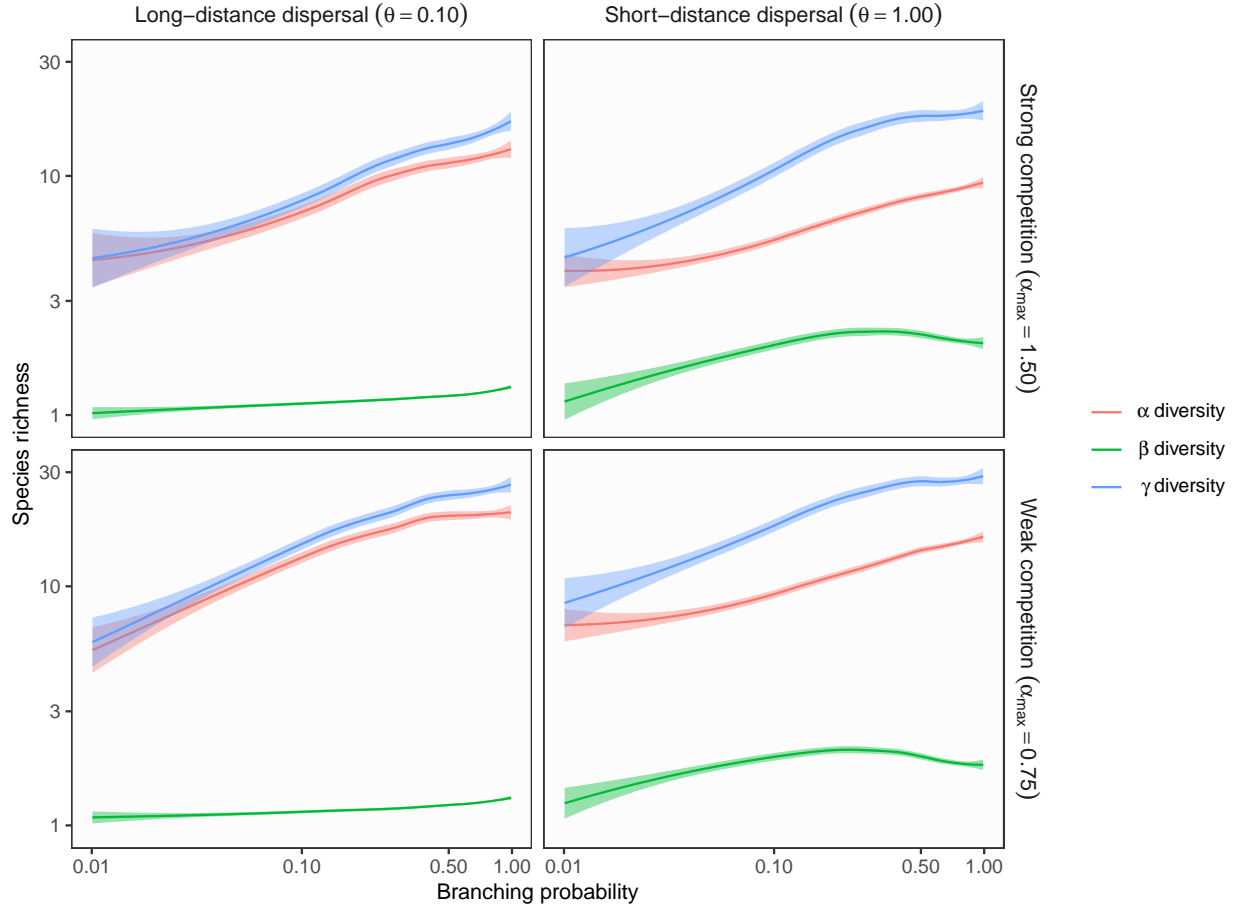


**Figure S8** Theoretical predictions for ecosystem complexity influences (branching probability) on  $\alpha$ ,  $\beta$ , and  $\gamma$  diversity in branching networks. In this simulation, environmental variation at headwaters ( $\sigma_h$ ) exceeds local environmental noise ( $\sigma_l$ ). Lines and shades are loess curves fitted to simulated data and its 95% confidence intervals. Each panel represents different ecological scenarios under which metacommunity dynamics were simulated. Rows represent different competition strength. Competitive coefficients ( $\alpha_{ij}$ ) were varied randomly from 0 to 1.5 (top, strong competition) or 0.75 (bottom, weak competition). Columns represent different dispersal scenarios. Two dispersal parameters were chosen to simulate scenarios with long-distance (the rate parameter of an exponential dispersal kernel  $\theta = 0.10$ ) and short-distance dispersal ( $\theta = 1.0$ ). Other parameters are as follows: dispersal probability  $p_d = 0.1$ ; environmental variation at headwaters  $\sigma_h = 1$ ; local environmental noise  $\sigma_l = 0.01$ .

**Figure S9 Influence of ecosystem complexity ( $p_d = 0.1$ ,  $\sigma_h = 1$ ,  $\sigma_l = 1$ )**

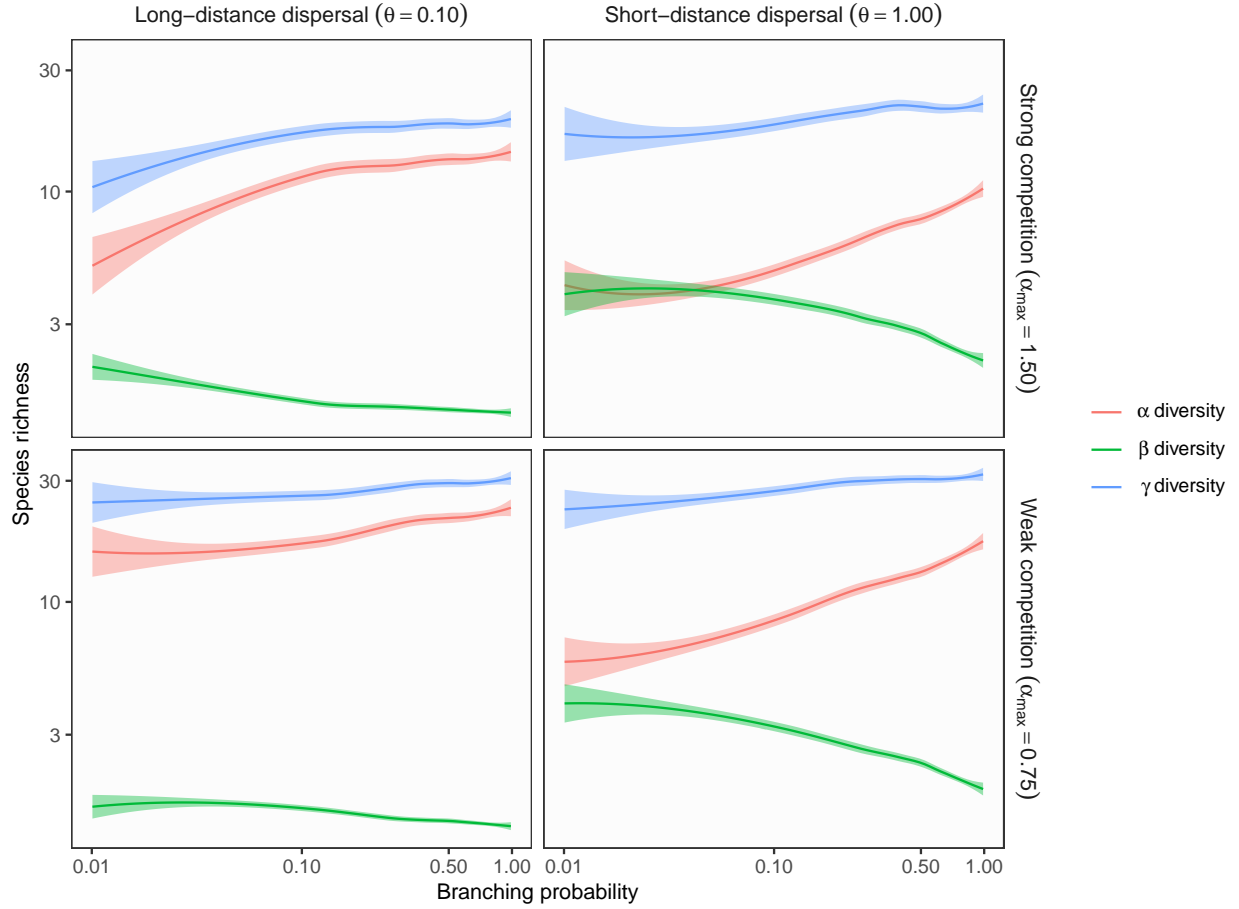


**Figure S9** Theoretical predictions for ecosystem complexity influences (branching probability) on  $\alpha$ ,  $\beta$ , and  $\gamma$  diversity in branching networks. In this simulation, environmental variation at headwaters ( $\sigma_h$ ) is equal to local environmental noise ( $\sigma_l$ ). Lines and shades are loess curves fitted to simulated data and its 95% confidence intervals. Each panel represents different ecological scenarios under which metacommunity dynamics were simulated. Rows represent different competition strength. Competitive coefficients ( $\alpha_{ij}$ ) were varied randomly from 0 to 1.5 (top, strong competition) or 0.75 (bottom, weak competition). Columns represent different dispersal scenarios. Two dispersal parameters were chosen to simulate scenarios with long-distance (the rate parameter of an exponential dispersal kernel  $\theta = 0.10$ ) and short-distance dispersal ( $\theta = 1.0$ ). Other parameters are as follows: dispersal probability  $p_d = 0.1$ ; environmental variation at headwaters  $\sigma_h = 1$ ; local environmental noise  $\sigma_l = 1$ .

**Figure S10** Influence of ecosystem complexity ( $p_d = 0.1$ ,  $\sigma_h = 0.01$ ,  $\sigma_l = 0.01$ )

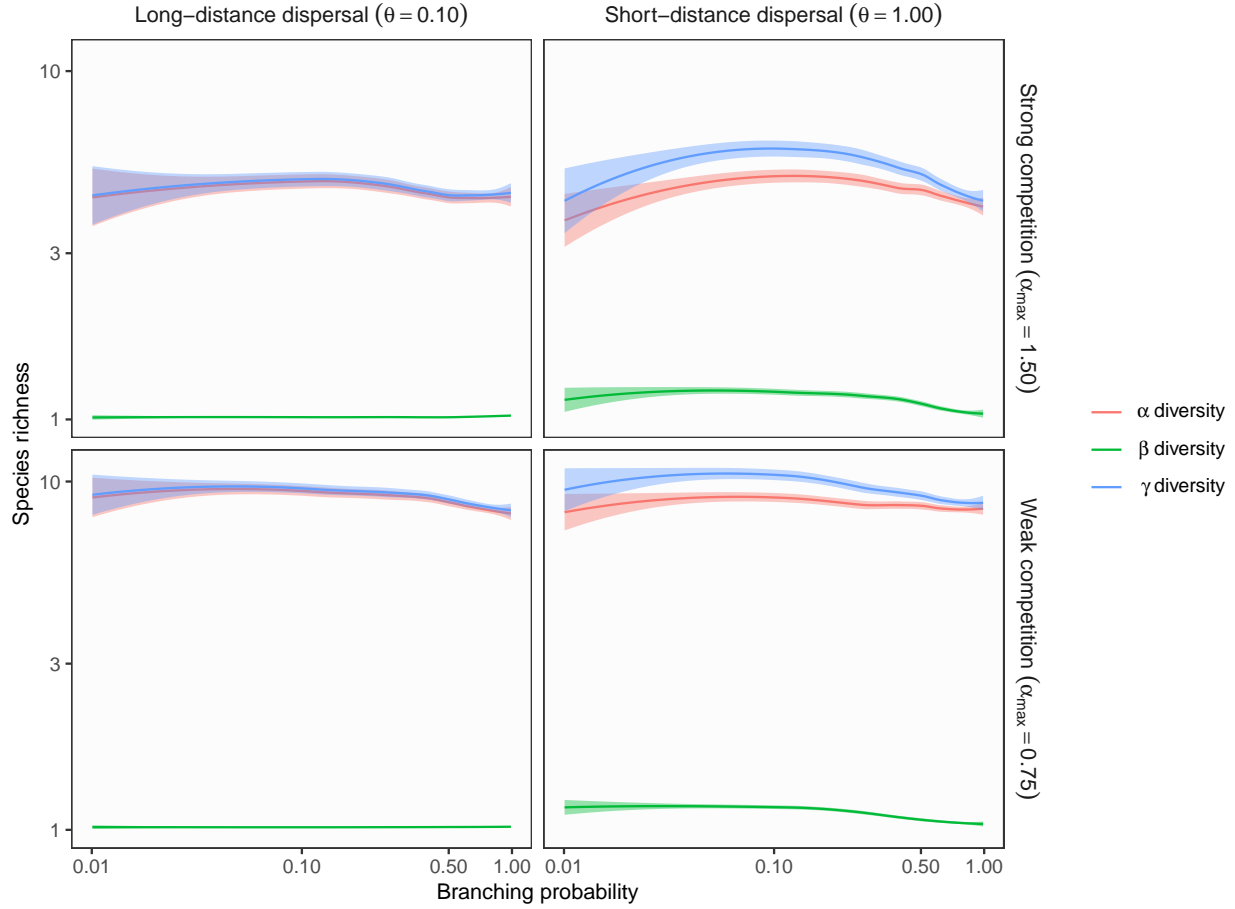


**Figure S10** Theoretical predictions for ecosystem complexity influences (branching probability) on  $\alpha$ ,  $\beta$ , and  $\gamma$  diversity in branching networks. In this simulation, environmental variation at headwaters ( $\sigma_h$ ) is equal to local environmental noise ( $\sigma_l$ ). Lines and shades are loess curves fitted to simulated data and its 95% confidence intervals. Each panel represents different ecological scenarios under which metacommunity dynamics were simulated. Rows represent different competition strength. Competitive coefficients ( $\alpha_{ij}$ ) were varied randomly from 0 to 1.5 (top, strong competition) or 0.75 (bottom, weak competition). Columns represent different dispersal scenarios. Two dispersal parameters were chosen to simulate scenarios with long-distance (the rate parameter of an exponential dispersal kernel  $\theta = 0.10$ ) and short-distance dispersal ( $\theta = 1.0$ ). Other parameters are as follows: dispersal probability  $p_d = 0.1$ ; environmental variation at headwaters  $\sigma_h = 0.01$ ; local environmental noise  $\sigma_l = 0.01$ .

**Figure S11** Influence of ecosystem complexity ( $p_d = 0.1$ ,  $\sigma_h = 0.01$ ,  $\sigma_l = 1$ )

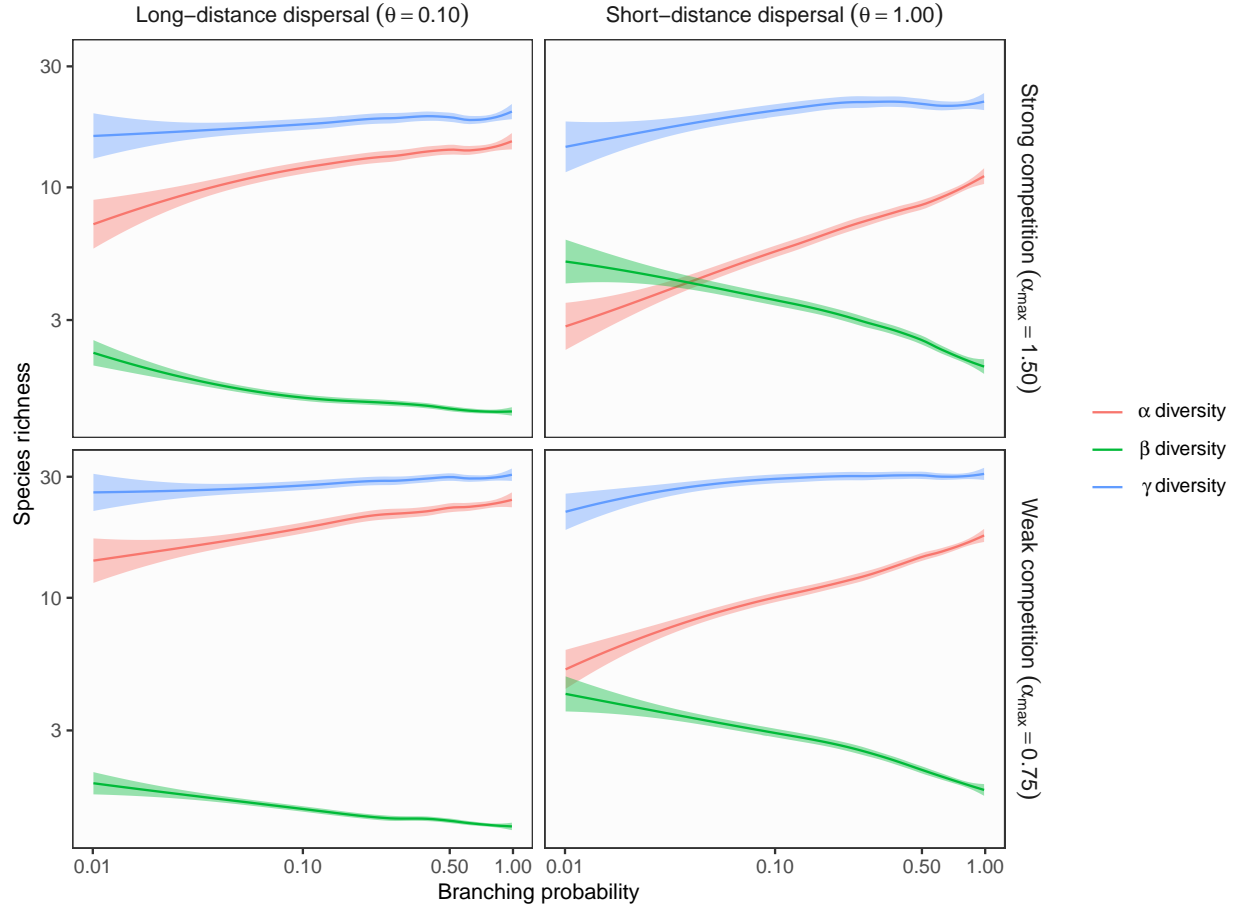


**Figure S11** Theoretical predictions for ecosystem complexity influences (branching probability) on  $\alpha$ ,  $\beta$ , and  $\gamma$  diversity in branching networks. In this simulation, environmental variation at headwaters ( $\sigma_h$ ) is less than local environmental noise ( $\sigma_l$ ). Lines and shades are loess curves fitted to simulated data and its 95% confidence intervals. Each panel represents different ecological scenarios under which metacommunity dynamics were simulated. Rows represent different competition strength. Competitive coefficients ( $\alpha_{ij}$ ) were varied randomly from 0 to 1.5 (top, strong competition) or 0.75 (bottom, weak competition). Columns represent different dispersal scenarios. Two dispersal parameters were chosen to simulate scenarios with long-distance (the rate parameter of an exponential dispersal kernel  $\theta = 0.10$ ) and short-distance dispersal ( $\theta = 1.0$ ). Other parameters are as follows: dispersal probability  $p_d = 0.1$ ; environmental variation at headwaters  $\sigma_h = 0.01$ ; local environmental noise  $\sigma_l = 1$ .

**Figure S12** Influence of ecosystem complexity ( $p_d = 0.01$ ,  $\sigma_h = 1$ ,  $\sigma_l = 1$ )

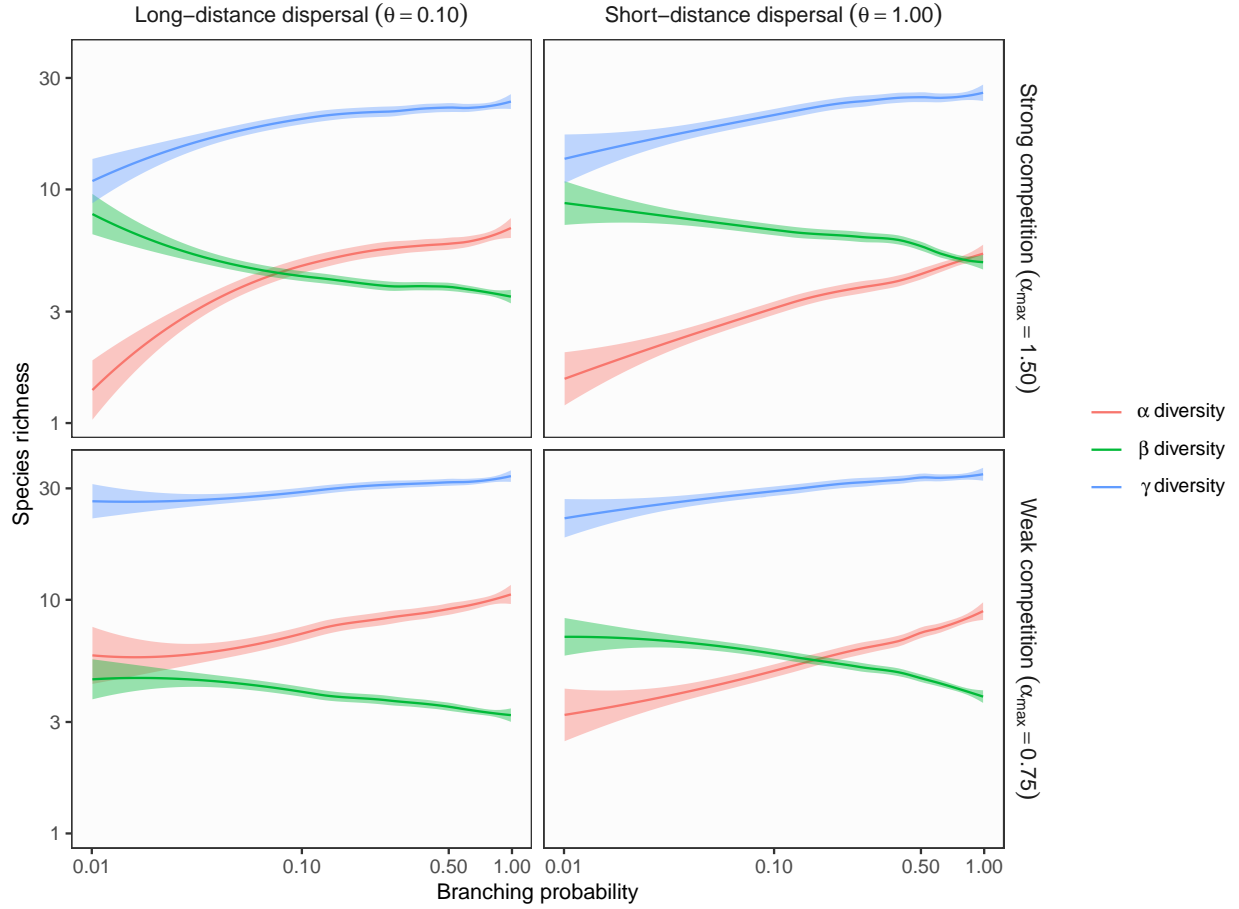


**Figure S12** Theoretical predictions for ecosystem complexity influences (branching probability) on  $\alpha$ ,  $\beta$ , and  $\gamma$  diversity in branching networks. In this simulation, environmental variation at headwaters ( $\sigma_h$ ) is equal to local environmental noise ( $\sigma_l$ ). Lines and shades are loess curves fitted to simulated data and its 95% confidence intervals. Each panel represents different ecological scenarios under which metacommunity dynamics were simulated. Rows represent different competition strength. Competitive coefficients ( $\alpha_{ij}$ ) were varied randomly from 0 to 1.5 (top, strong competition) or 0.75 (bottom, weak competition). Columns represent different dispersal scenarios. Two dispersal parameters were chosen to simulate scenarios with long-distance (the rate parameter of an exponential dispersal kernel  $\theta = 0.10$ ) and short-distance dispersal ( $\theta = 1.0$ ). Other parameters are as follows: dispersal probability  $p_d = 0.01$ ; environmental variation at headwaters  $\sigma_h = 1$ ; local environmental noise  $\sigma_l = 1$ .



**Figure S13 Influence of ecosystem complexity ( $p_d = 0.01$ ,  $\sigma_h = 0.01$ ,  $\sigma_l = 0.01$ )**

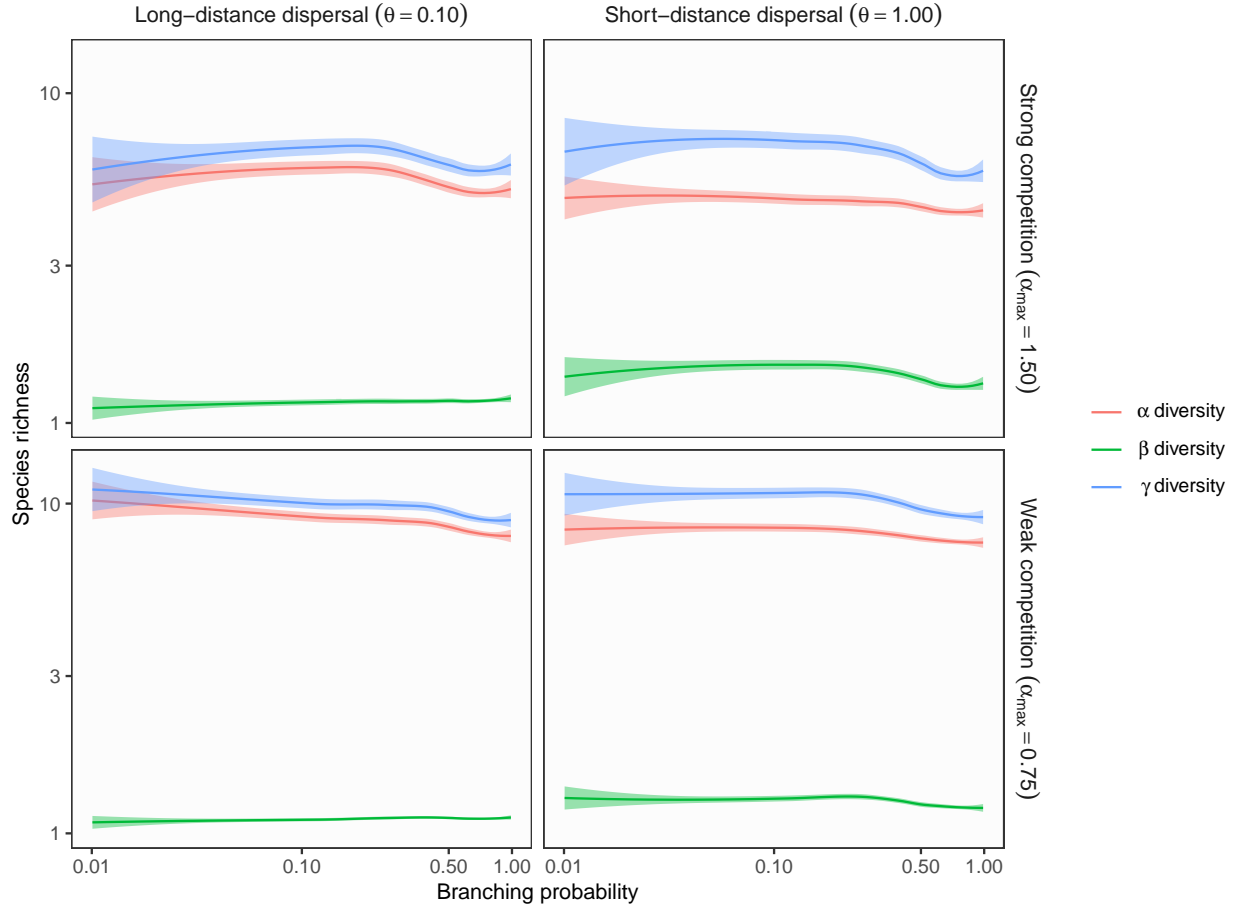


**Figure S13** Theoretical predictions for ecosystem complexity influences (branching probability) on  $\alpha$ ,  $\beta$ , and  $\gamma$  diversity in branching networks. In this simulation, environmental variation at headwaters ( $\sigma_h$ ) is equal to local environmental noise ( $\sigma_l$ ). Lines and shades are loess curves fitted to simulated data and its 95% confidence intervals. Each panel represents different ecological scenarios under which metacommunity dynamics were simulated. Rows represent different competition strength. Competitive coefficients ( $\alpha_{ij}$ ) were varied randomly from 0 to 1.5 (top, strong competition) or 0.75 (bottom, weak competition). Columns represent different dispersal scenarios. Two dispersal parameters were chosen to simulate scenarios with long-distance (the rate parameter of an exponential dispersal kernel  $\theta = 0.10$ ) and short-distance dispersal ( $\theta = 1.0$ ). Other parameters are as follows: dispersal probability  $p_d = 0.01$ ; environmental variation at headwaters  $\sigma_h = 0.01$ ; local environmental noise  $\sigma_l = 0.01$ .

**Figure S14 Influence of ecosystem complexity ( $p_d = 0.01$ ,  $\sigma_h = 0.01$ ,  $\sigma_l = 1$ )**

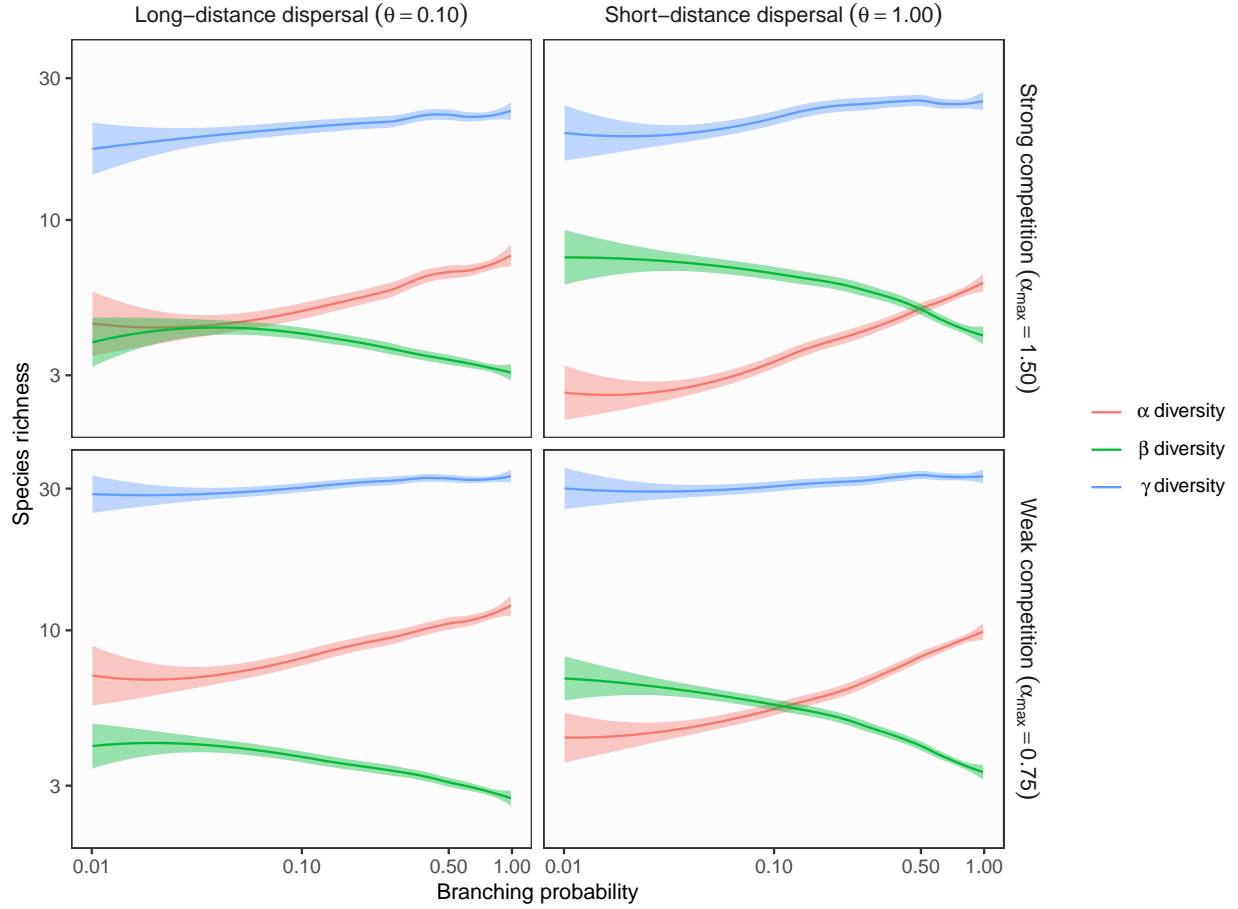


**Figure S14** Theoretical predictions for ecosystem complexity influences (branching probability) on  $\alpha$ ,  $\beta$ , and  $\gamma$  diversity in branching networks. In this simulation, environmental variation at headwaters ( $\sigma_h$ ) is less than local environmental noise ( $\sigma_l$ ). Lines and shades are loess curves fitted to simulated data and its 95% confidence intervals. Each panel represents different ecological scenarios under which metacommunity dynamics were simulated. Rows represent different competition strength. Competitive coefficients ( $\alpha_{ij}$ ) were varied randomly from 0 to 1.5 (top, strong competition) or 0.75 (bottom, weak competition). Columns represent different dispersal scenarios. Two dispersal parameters were chosen to simulate scenarios with long-distance (the rate parameter of an exponential dispersal kernel  $\theta = 0.10$ ) and short-distance dispersal ( $\theta = 1.0$ ). Other parameters are as follows: dispersal probability  $p_d = 0.01$ ; environmental variation at headwaters  $\sigma_h = 0.01$ ; local environmental noise  $\sigma_l = 1$ .

## References

1. Fukushima, M., Kameyama, S., Kaneko, M., Nakao, K. & Ashley Steel, E. Modelling the effects of dams on freshwater fish distributions in Hokkaido, Japan. *Freshwater Biology* **52**, 1511–1524 (2007).
2. Comte, L. *et al.* RivFishTIME: A global database of fish time-series to study global change ecology in riverine systems. *Global Ecology and Biogeography* **30**, 38–50 (2021).
3. Terui, A. *et al.* Metapopulation stability in branching river networks. *Proceedings of the National Academy of Sciences* **115**, E5963–E5969 (2018).
4. Terui, A. & Miyazaki, Y. Three ecological factors influencing riverine fish diversity in the Shubuto River system, Japan: Habitat capacity, habitat heterogeneity and immigration. *Limnology* **17**, 143–149 (2016).